Thermochimica Acta 666 (2018) 60–65

Contents lists available at ScienceDirect

Thermochimica Acta

journal homepage: www.elsevier.com/locate/tca

# Reaction mechanism of Al-CuO nanothermites with addition of multilayer graphene

Jinpeng Shen[a], Zhiqiang Qiao[c], Jun Wang[c], Guangcheng Yang[c], Jin Chen[c], Zhaoqian Li[b], Xin Liao[a,*], Haiyang Wang[d], Michael R. Zachariah[d]

[a] School of Chemical Engineering, Nanjing University of Science and Technology, Nanjing, 210094, Jiangsu, China
[b] State Key Laboratory of Environment-Friendly Energy Materials, Southwest University of Science and Technology, Mianyang, 621010, Sichuan, China
[c] Institute of Chemical Materials, China Academy of Engineering Physics, Mianyang, 621900, Sichuan, China
[d] Department of Chemical and Biomolecular Engineering, University of Maryland, College Park, MD 20742, United States

ARTICLE INFO

*Keywords:*
Multilayer graphene
Al-CuO nanothermites
CuO-C reaction
Al—C bond
Reaction mechanism

ABSTRACT

Reactions of nanothermites is complex, and the heterogeneous reaction poorly understood. In this study Al-CuO-multilayer graphene (MLG) composites were studied to explore the effects of MLG on the reaction properties, products composition and reaction mechanism of Al-CuO nanothermites. The morphology composition of Al-CuO-MLG composites before and after reaction was studied by scanning electron microscope (SEM). And detailed reaction pathways were characterized by X-ray diffraction (XRD), thermal gravimetric analysis and differential scanning calorimeter (TG-DSC) and X-ray photoelectron spectroscopy (XPS). Results indicate that the presence of MLG between nano-Al and nano-CuO particles tunes and improves reaction characteristics. A total heat of reaction of the Al-CuO-MLG (1 wt%) composites is 1679 J/g, increased by ~87.5 J/g compared to that of Al-CuO composites.

## 1. Introduction

The nanothermites [1–4] have received increasing interest over the past 15 years for additives in propellants and explosive, combustion synthesis of advanced materials [5,6], and on-chip energetics [7].

One of area of interest is how to moderate or tune reactive properties of the thermites. This could include changing oxidizers that have different oxygen release temperatures [8,9], mixtures of fuels that have different reaction thresholds [10,11] or other additives that might change the physical properties of the mixture. Graphene exhibits intriguing electronic, optical and thermal conduction properties [12,13] and has been widely used as promising thermal interface materials [14,15]. The reported thermal conductivity of multilayer graphene (MLG) is in the range of 4,840-5,300 $W\ m^{-1}\ K^{-1}$ at room temperature, which is significantly above in-plane bulk graphite for (2000 $W\ m^{-1} K^{-1}$) [16–18]. In a recent study it was found that the addition of graphene can increase the thermal conductivity of Al/Teflon by 98% [19] and enhance the burning rate of solid propellant by 100% [20]. Moreover, Thiruvengadathan et al. [21] reported a method for directing the self-assembly of Al-$Bi_2O_3$ nanothermite with graphene oxide. The results demonstrated the benefits of self-assembly and the role of graphene oxide as an energetic reactant. The Al-$Bi_2O_3$ nanothermite with 5 wt % graphene oxide showed a remarkable enhancement in energy release from 739 ± 18 to 1421 ± 12 J/g. Classical theory of laminar flames shows that the propagation velocity scales as the product of thermal conductivity and reaction rate to the ½ power. Egan et al. [22] did an analysis that showed that the thermal conductivity in a mixture was not sufficient to conduct enough energy to explain the propagation velocity commonly observed. The addition of graphene or other high conductivity material may offer insights into reaction mechanism or alternatively lead to new strategies for moderating combustion rate.

Here we demonstrate a unique methodology using MLG with high thermal conductivity as thermal interface material between the fuel and oxidizer to tune the combustion reactivity of the nanothermite. The potential microscopic mechanisms of combustion reaction were investigated using a host of characterization techniques including scanning electron microscope (SEM), X-ray diffraction (XRD), Thermal gravimetric analysis and differential scanning calorimeter (TG-DSC), and X-ray photoelectron spectroscopy (XPS). The detailed reaction mechanism of the Al-CuO-MLG composites can be well described.

* Corresponding author.
*E-mail address:* liaoxin331@163.com (X. Liao).

https://doi.org/10.1016/j.tca.2018.06.005
Received 18 April 2018; Received in revised form 7 June 2018; Accepted 8 June 2018
Available online 14 June 2018

**Table 1**
Experimental parameters used in the synthesis of Al-CuO-multilayer graphene (MLG) composites.

| Sample | 1 | 2 | 3 | 4 | 5 | 6 |
|---|---|---|---|---|---|---|
| MLG per total solid content (wt %) | 0 | 1 | 2 | 3 | 5 | 10 |
| Al-CuO nanothermites per total solid content (wt %) | 100 | 99 | 98 | 97 | 95 | 90 |

## 2. Experimental

### 2.1. Materials preparation

Al nanoparticles procured from Guangzhou Hongwu materials technology co. LTD, China. MLG was obtained from Institute of Coal Chemistry, Chinese Academy of Sciences with a purity of 99.9 wt%. Diameters ranged from 50 nm to 200 nm, and the active Al content was 80 wt% (mass fraction) with a 2–5 nm aluminum oxide shell. The nano-CuO was prepared using microwave synthesis with a purity of 99 wt% [23]. The Al-CuO nanothermites was prepared to have a stoichiometric ratio with 22 wt% nano-Al and 78 wt% nano-CuO. MLG was added from 1% to 10% by mass (Table 1). In order to ensure mixing uniformity, nano-Al, nano-CuO and MLG were mixed in hexane by sonicating for 10 min followed by magnetic stirring for 10 min. The process was repeated three times. In addition, CuO with 50 wt% MLG were prepared similarly. All the Al-CuO-MLG composites were dried under vacuum at 50 °C.

In order to identify reaction pathways, Al-MLG (3 wt%), Al-CuO and Al-CuO-MLG (3 wt%) under ambient conditions were ignited using a needle of electric ignitor in a pressure cell under ambient conditions. Reaction products of them were collected for SEM, XRD and XPS analysis.

### 2.2. Materials characterization

The morphology and dimensions of the nanostructures in the composites were observed by SEM (ZEISS Ultra-55, Carl Zeiss Meditec AG, Jena, Germany). The sample was placed on double-sided tape and then observed using field SEM at an acceleration voltage of 10–15 kV after gold sputtering coating under the vacuum degree of $10^{-6}$ Pa for 120 s. The chemical composition of the composites was characterized using XRD (X'Pert PRO, PANalytical, Almelo, the Netherlands) analysis with Cu-Ka ($\lambda = 1.54059$ Å) radiation at 50 kV and 30 mA, and a monochromatic graphite diffracted beam. The samples were packed into an amorphous silicon holder, and the diffraction angle (2θ) was scanned from 5° to 80°, and the scanning rate was 10° $min.^{-1}$. Raman spectrum of Al-CuO nanothermite with different wt% MLG were recorded by using a Renishaw InVia Raman microscope with an excitation wavelength of $\lambda = 514$ nm. And the results of Raman are shown in Figure S1. The thermal properties were tested by TG-DSC (NETZSCH STA 449F3), recording with 50 mL·$min^{-1}$ Ar at 10 °C·$min^{-1}$ from 50 to 1000 °C. XPS analysis was recorded on an ESCALAB 250 XPS X-ray electron spectrometer (American Thermo Electron Corporation).

## 3. Results and discussion

### 3.1. Morphology of the Al/CuO/MLG composites

SEM images of MLG, nano-Al, nano-CuO and Al-CuO with 3 wt% MLG are shown in Fig. 1. The MLG seen in Fig. 1a is seen to be the range of tens of micrometers, and many wrinkles and voids (complete image set in Figure S2). The thickness of MLG is about 10 nm with about 20 layers [24,25]. The average particle diameter of Al is 50–150 nm (Fig. 1(b, (c) and (e)) show the nano-CuO synthesized by the microwave method, indicating a rod-like structure, with the average length, width and thickness of each nano-CuO rod are about 2 μm, 200 nm and 50 nm, respectively. Fig. 1(d) and 1(e) are the low and high resolution SEM micrographs of the Al-CuO with 3 wt% MLG, which show loose powder with considerable void space (complete image set in Figure S3). Fig. 1(f) shows the morphology of reaction products of Al-CuO with 3 wt% MLG. As expected we see considerable increase in particle size as a result of reactive sintering [26], although we can still see some intact MLG flakes (box in image).

### 3.2. Product of the Al/CuO/MLG composites

Fig. 2 shows the XRD pattern of the reaction products of Al-CuO with 3 wt% MLG, which exhibits peaks of Cu, $Cu_2O$, α-$Al_2O_3$, δ-$Al_2O_3$, $Al_2Cu$ and $CuAlO_2$. Moreover, most of the alumina might be amorphous as the broad peak shown in Fig. 2. Based on the observed products we can write an overall reaction in Eq. (1). Interestingly $Al_2Cu$, has seldom previously been reported nor is it expected on thermodynamic grounds [27,28] for a pure Al/CuO thermite. In the next section XPS analysis further confirms the presence of the $Al_2Cu$ alloy. It is evident that the

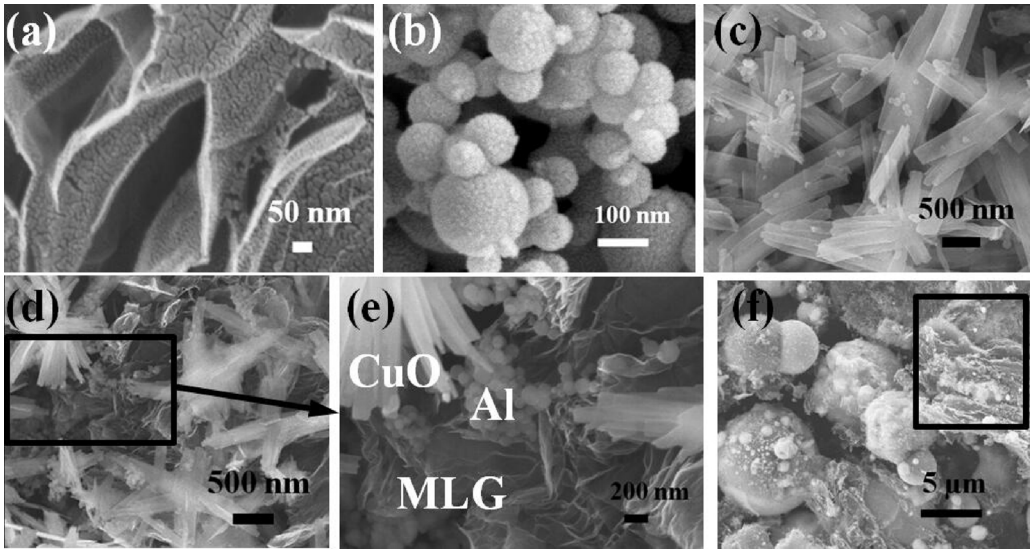


**Fig. 1.** SEM images of (a) multilayer graphene (MLG), (b) nano-Al, (c) nano-CuO and (d) Al-CuO with 3 wt% MLG, (e) magnification of a part of (d), (f) reaction products of Al-CuO with 3 wt% MLG.

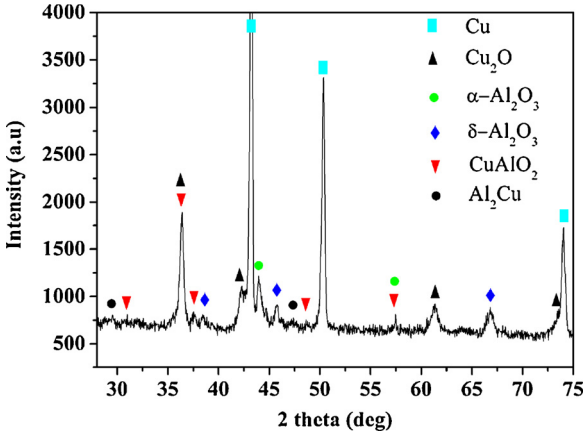


**Fig. 2.** XRD of the reaction products of Al-CuO with 5 wt% multilayer graphene.

reaction paths of Al-CuO-MLG composites are different from that of the Al-CuO nanothermites. Moreover, $CuAlO_2$ can be formed from the reactions of $Cu_2O$ with $Al_2O_3$ (as shown in Eq. (2) [29,30]) and CuO with $Al_2O_3$ (as shown in Eq. (3) [31,32]). The detailed reaction between Al, CuO and C (MLG), especially Al-C and CuO-C, are examined more throughly with TG-DSC and XPS in the next section.

$$5Al+6CuO \rightarrow 2Cu+Cu_2O+Al_2O_3+CuAlO_2+Al_2Cu \quad (1)$$

$$Cu_2O+Al_2O_3 \rightarrow 2CuAlO_2 \quad (2)$$

$$2CuO+Al_2O_3 \rightarrow 2CuAlO_2+1/2O_2 \quad (3)$$

### 3.3. Thermal analyses of Al/CuO/MLG composites

The thermal properties of the Al-CuO-MLG composites are characterized by TG-DSC and shown in Fig. 3 and Table 2. There are two major exothermic peaks and one endothermic peak associated with the thermite reaction [31]. With MLG increasing from 0 wt% to 10 wt%, the first exothermic peak is observed with a similar temperature of 590 °C. This means that the nanothermites have reacted prior to the melting of Al (660.0 °C) in a condensed phase process [33]. Following the first exothermic peak, a small endothermic peak is observed at around 658 °C, which is attributed to the melting of unreacted Al. The second exothermic peak, caused by the reaction of the melted unreacted Al with $Cu_2O$ and some CuO [31], is lowered from 711 °C to 684 °C with the increase of MLG from 1 wt% to 10 wt %. The decreasing trend is closely related to the high thermal conductivity of MLG. The thermal conductivity of the Al-CuO-MLG composites increases with the increase of MLG from 0 wt% to 10 wt% at the same temperature (see Supporting Information, Figure S4). The second exothermic peaks of Al-CuO-MLG composites second reaction can be mainly described by liquid (Al)-solid ($Cu_2O$ and CuO) diffusion mechanism [34,35], which are higher than

**Table 2**
Summarized results for DSC experiments of Al-CuO-nanothermites with different proportions of multilayer graphene (MLG).

| Sample | MLG (wt %) | $T_{exo1}$ (°C) | $T_{endo}$ (°C) | $T_{exo2}$ (°C) | $\triangle H_{total}$ (J/g) |
|---|---|---|---|---|---|
| 1 | 0% | 596 | 658 | 677 | 1591.5 ± 26.2 |
| 2 | 1% | 596 | 658 | 711 | 1679.0 ± 22.6 |
| 3 | 2% | 596 | 658 | 706 | 1652.5 ± 31.8 |
| 4 | 3% | 595 | 658 | 704 | 1530.0 ± 42.4 |
| 5 | 5% | 595 | 659 | 698 | 1489.5 ± 57.3 |
| 6 | 10% | 595 | 659 | 684 | 1465.0 ± 49.5 |

Nitice: $T_{exo1}$: Temperature of the first exothermic, $T_{exo2}$: Temperature of the second exothermic, $T_{endo}$: Temperature of the endothermic, $\triangle H_{total}$: Total of energy release.

the peak (677 °C) of the Al-CuO without MLG. The main reason is that addition of loose MLG increase the mass diffusion and heat transfer length between the reactants.

Moreover, the Al-C reaction is potentially another reaction pathway in addition to solid-solid and liquid-solid diffusion reactions in the Al-CuO reaction process. According to Fig. 3(b), there is a small exothermic peak at 665 °C due to Al-C reactions [22], described with XPS in more detail in the next section. The total of energy release (ΔH) of each Al-CuO-MLG composites is shown in Table 2. The maximum energy release was observed for 1 wt% MLG, with a value of 1679 J/g, which is an increase of ~87.5 J/g compared to that of Al-CuO composites.

Fig. 3(c) shows the TG results of Al-CuO nanothermites with MLG. We can see that Al-CuO reaction without MLG has almost no mass loss. The weight-loss of the Al-CuO-MLG composites increases with the increase of MLG from 1 wt% to 10 wt%. Because almost no gas is released according to Eq. (1), there must have been other reaction. Further, the reaction of CuO and MLG is investigated as shown in Fig. 4. There are one (curve 1) and two (curve 2) evident weight losses in Fig. 4(a), refered to CuO and CuO-MLG composites, respectively. There is a broad and flat peak from 450 °C to 600 °C in Fig. 4(b). The energy release of the MLG and CuO reaction is 1166 J/g. An endothermic peak is observed at 886 °C, which is refereed to the decomposition of CuO. And the theoretical reaction of MLG and CuO is shown by Eq. (4). Moreover, CuO decomposes to $Cu_2O$ and $O_2$ at 918 °C by Eq. (5) which is reported previously [36,37]. The decomposition temperature reduces by 32 °C due to adding the MLG. The TG-DSC results indicate that the reaction characteristics between nano-Al and CuO particles can be improved after adding MLG.

$$C+4CuO \rightarrow 2Cu_2O+CO_2 \quad (4)$$

$$4CuO \rightarrow 2Cu_2O+O_2 \quad (5)$$

### 3.4. XPS analyses for reaction pathway

To better understand the reaction mechanism of Al-CuO-MLG, and particularly the Al-C reactions, XPS are used to investigate the chemical

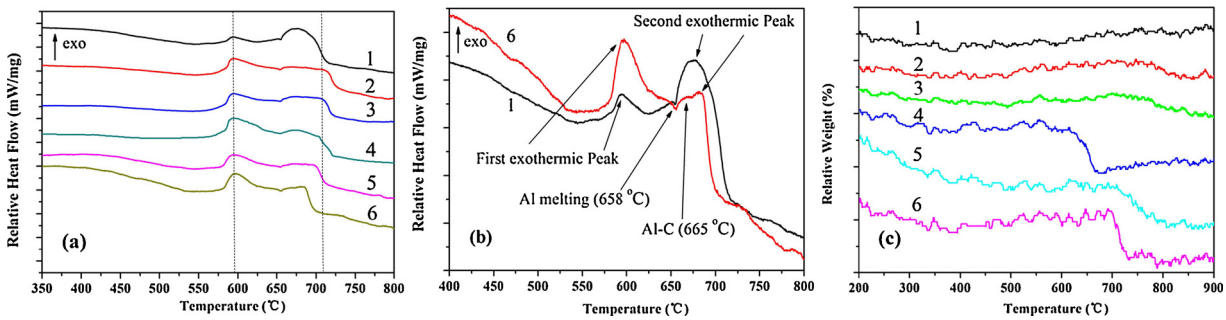


**Fig. 3.** DSC curves of (a) Al-CuO nanothermites with: (1) 0 wt% multilayer graphene (MLG), (2) 1 wt% MLG, (3) 2 wt% MLG, (4) 3 wt% MLG, (5) 5 wt% MLG, (6) 10 wt% MLG and (b) detailed reaction peaks of Al-CuO nanothermites with 0% MLG and 10 wt% MLG. (c) TG curves of the Al-CuO-MLG composites.

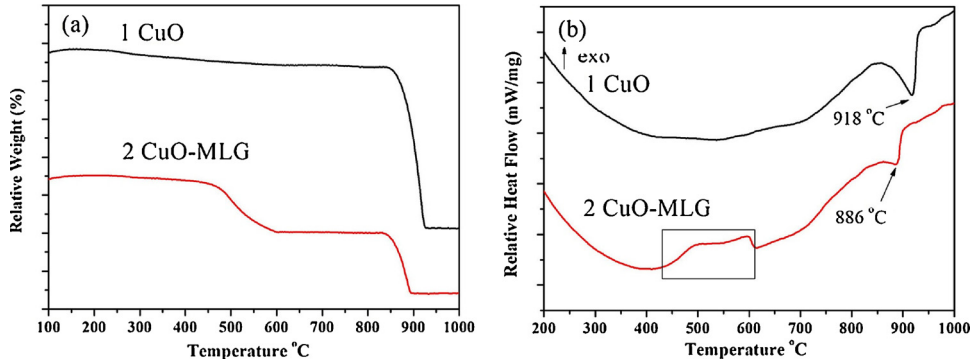


**Fig. 4.** TG-DSC curves of (1) CuO, (2) CuO with 50 wt% MLG.

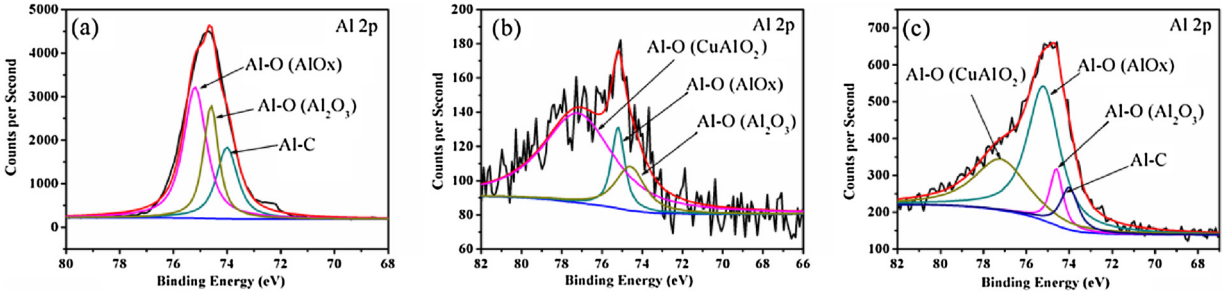


**Fig. 5.** XPS Al 2p spectra of reaction products: (a) Al with 3 wt% multilayer graphene (MLG), (b) Al-CuO, (c) Al-CuO with 3 wt% MLG.

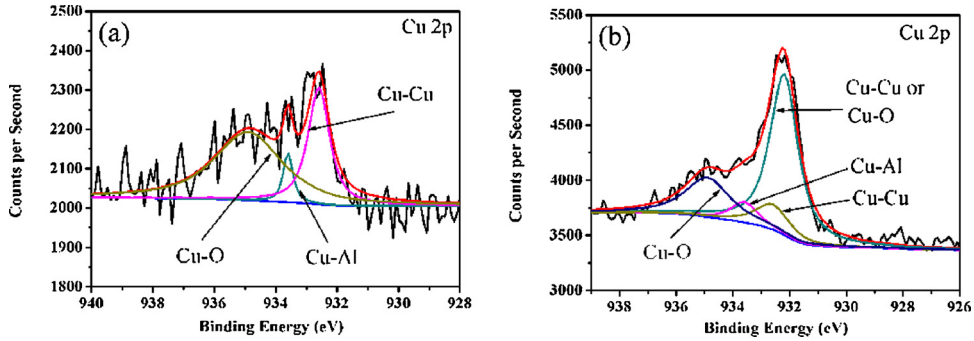


**Fig. 6.** XPS Cu 2p spectra of (a) reaction products of Al-CuO, (b)reaction products of Al-CuO with 3 wt% multilayer graphene.

evolution of reaction products. The Al 2p spectrums of reaction products of Al with 3 wt% MLG, Al-CuO and Al-CuO with 3 wt% MLG are shown in Fig. 5 and the peak assignments are listed in Table S1 according to the handbook of X-Ray photoelectron spectroscopy [38]. Our observed binding energy of 75.2 eV, 74.6 eV and 77.2 eV are consistent with peaks of Al-O ($AlO_x$), Al-O ($Al_2O_3$) and Al-O ($CuAlO_2$) [39], respectively. The existence of Al-C is confirmed with the binding energy of 74.0 eV [40]. Bartolucci et al. [41] observed that when 0.1 wt% graphene was employed to create Al-graphene composite at 550 °C for 4 h, strong peaks for aluminum carbide ($Al_4C_3$) was observed, as is shown in Eq. (6). However we see no evidence of $Al_4C_3$ in our XRD results (see Fig. 2). It may be resulted from the amorphous Al-C phase.

$$\text{A1 (1)} + \text{C} \rightarrow \text{AlxCy (amorphous)} \quad (6)$$

Furthermore, the spectrums of Cu 2p in Fig. 6 and Table S2, also confirms the existence of a Cu-Al ($Al_2Cu$) alloy at a binding energy of 933.6 eV [38]. And the pure Cu 2p core levels at 932.2 eV and 932.6 eV, respectively. The peak at 932.2 eV could also consider the possibility of the presence of CuO ($Cu_2O$). Moreover, a new peak at 934.9 eV for reaction products of both Al-CuO (see Fig. 6(a)) and Al-CuO-MLG (see Fig. 6(b)), and it associated with an Cu-O ($CuAl_2O_4$) [42,43], which is not detected in the reaction product by XRD. According to Cai [44], $CuAl_2O_4$ is synthesized by CuO-$Al_2O_3$ reaction and then decomposed into $CuAlO_2$, $Al_2O_3$ and $O_2$. Thus $CuAl_2O_4$ is not fully decomposed here. To further confirm the detailed reaction process, more reliable experimental and characterizations will conduct later.

### 3.5. Reaction mechanism of Al-CuO-MLG composites

According to the above results of XRD, TG-DSC and XPS, the reaction pathways for the Al-CuO-MLG composites with increasing temperatures are summarized in Table 3. According to the reaction temperature, we proposed a three-stage reaction mechanism to describe the reaction pathways. It is similar to the oxidation process of the nano Al powder and decomposition of the CuO nanoparticles, reported by Wen group [45,46]. First, this stage is a exothermic stage, including Al (solid)-CuO reaction and CuO-C reaction from 450 °C to 650 °C. Second, the stage is caused by the melting of the nano-Al about 660 °C. Third, there are multistep reactions in the exothermic stage from 660 °C to 800 °C, including $Cu_2O$-$Al_2O_3$ reaction, CuO-$Al_2O_3$ reaction, Al(liquid)-C reaction, Al(liquid)-CuO reaction and Al(liquid)-$Cu_2O$ reaction.

**Table 3**
List of proposed reaction pathways for Al-CuO-multilayer graphene (MLG) composites observed at different temperatures.

| Stage | T (°C) | Reactions | Equations |
|---|---|---|---|
| 1 | 450-650 | $5Al(l)+6CuO \rightarrow 2Cu+Cu_2O+Al_2O_3+CuAlO_2+Al_2Cu$ | (1) |
| | | $C+4CuO \rightarrow 2Cu_2O+CO_2$ | (4) |
| 2 | 650-660 | Al melting point | |
| 3 | 660-800 | $2Al(l)+3Cu_2O \rightarrow Al_2O_3+6Cu$ | (2) |
| | | $2CuO+Al_2O_3 \rightarrow 2CuAlO_2+1/2O_2$ | (3) |
| | | $Al(l)+C \rightarrow AlxCy$(amorphous) | |
| | | $Al(l)+CuO$ [31] | |
| | | $2Al(l)+3Cu_2O \rightarrow Al_2O_3+6Cu$ [47] | |

Notices: s-solid, l-liqud. T: Reaction temperature.

## 4. Conclusions

The Al-CuO-MLG composites are fabricated by physical mixing method and the reaction mechanism of Al-CuO-MLG was systemically investigated. Firstly, the presence of Al-C chemical bonds in the reaction products was confirmed by TG/DSC and XPS. And the results indicated the reaction products include Cu, $Cu_2O$, $\alpha$-$Al_2O_3$, $\delta$-$Al_2O_3$, $Al_2Cu$, Al-C component and $CuAlO_2$. And the results also showed different reaction paths of Al-CuO-MLG composites compared with that of the Al-CuO nanothermites, according to the formation of $Al_2Cu$ component in the Al-CuO-MLG reaction. Furthermore, with the addition of 1 wt% MLG, the energy release is increased by ~87.5 J/g compared to that of Al-CuO composites. With MLG increasing from 1 wt% to 10 wt%, the second exothermic peak is reduced from 710.9 °C to 684.0 °C. We propose a three-stage reaction mechanism to describe the multistep reaction pathways. Our study confirms that graphene improves the characteristics of the heterogeneous reaction process and energy release pathway of Al-CuO composites.

## Acknowledgments

This work is supported by the National Natural Science Foundation of China (Grant Nos. 11502247, 11502242, 11702268, and 51506093) and the Open Project of State Key Laboratory of Environment-friendly Energy Materials (No.14zxfk08) from Southwest University of Science and Technology.

## Appendix A. Supplementary data

Supplementary material related to this article can be found, in the online version, at doi:https://doi.org/10.1016/j.tca.2018.06.005.

## References

[1] K.S. Martirosyan, Nanoenergetic gas-generators: principles and applications, J. Mater. Chem. 21 (2011) 9400–9405.
[2] K.B. Plantier, M.L. Pantoya, A.E. Gash, Combustion wave speeds of nanocomposite Al/$Fe_2O_3$: the effects of $Fe_2O_3$ particle synthesis technique, Combust. Flame 140 (2005) 299–309.
[3] K.S. Martirosyan, L. Wang, A. Vicent, D. Luss, Synthesis and performance of bismuth trioxide nanoparticles for high energy gas generator use, Nanotechnology 20 (2009) 405609.
[4] E.L. Dreizin, Metal-based reactive nanomaterials, Prog. Energy Combust. 35 (2009) 141–167.
[5] A. Varma, A.S. Rogachev, A.S. Mukasyan, S. Hwang, Complex behavior of self-propagating reaction waves in heterogeneous media, Proc. Natl. Acad. Sci. U. S. A. 95 (1998) 11053–11058.
[6] Y. Liu, B. Gao, Z. Qiao, Y. Hu, W. Zheng, L. Zhang, Y. Zhou, G. Ji, G. Yang, Gram-scale synthesis of graphene quantum dots from single carbon atoms growth via energetic material deflagration, Chem. Mater. 27 (2015) 4319–4327.
[7] K. Zhang, C. Rossi, M. Petrantoni, N. Mauran, A nano initiator realized by integrating Al/CuO-based nanoenergetic materials with a Au/Pt/Cr microheater, J. Microelectromech. Syst. 17 (2008) 832–836.
[8] E. Shafirovich, C. Zhou, A.S. Mukasyan, A. Varma, G. Kshirsagar, Y. Zhang, J.C. Cannon, Combustion fluctuations in low-exothermic condensed systems for emergency oxygen generation, Combust. Flame 13 (2003) 557–561.
[9] L. Zhou, N. Piekiel, S. Chowdhury, M.R. Zachariah, Time-resolved mass spectrometry of the exothermic reaction between nanoaluminum and metal oxides: the role of oxygen release, J. Phys. Chem. C 114 (2010) 14269–14275.
[10] G. Jian, S. Chowdhury, K. Sullivan, M.R. Zachariah, Nanothermite reactions: Is gas phase oxygen generation from the oxygen carrier an essential prerequisite to ignition? Combust. Flame 160 (2013) 432–437.
[11] C. Wu, K. Sullivan, S. Chowdhury, G. Jian, L. Zhou, M.R. Zachariah, Encapsulation of perchlorate salts within metal oxides for application as nanoenergetic oxidizers, Adv. Funct. Mater. 22 (2012) 78–85.
[12] A.A. Balandin, Thermal properties of graphene and nanostructured carbon materials, Nat. Mater. 10 (2011) 569–581.
[13] A.A. Balandin, S. Ghosh, W. Bao, I. Calizo, D. Teweldebrhan, F. Miao, C. Lau, Superior thermal conductivity of single-layer graphene, Nano Lett. 8 (2008) 902–907.
[14] K.M.F. Shahil, A.A. Balandin, Graphene-multilayer graphene nanocomposites as highly efficient thermal interface materials, Nano Lett. 12 (2012) 861–867.
[15] R. Prasher, Thermal interface materials: historical perspective, status, and future directions, Proc. IEEE 94 (2006) 1571–1586.
[16] S. Park, R.S. Ruoff, Chemical methods for the production of graphenes, Nat. Nanotechnol. 4 (2009) 217–224.
[17] S. Ghosh, I. Calizo, D. Teweldebrhan, E.P. Pokatilov, D.L. Nika, A.A. Balandin, W. Bao, F. Miao, C.N. Lau, Extremely high thermal conductivity of graphene: prospects for thermal management applications in nanoelectronic circuits, Appl. Phys. Lett. 92 (2008) 151911.
[18] K. Kappagantula, M.L. Pantoya, E.M. Hunt, Impact ignition of aluminum-teflon based energetic materials impregnated with nano-structured carbon additives, J. Appl. Phys. 112 (2012) 024902.
[19] K. Kappagantula, M.L. Pantoya, Experimentally measured thermal transport properties of aluminum-polytetrafluoroethylene nanocomposites with graphene and carbon nanotube additives, Int. J. Heat Mass Transf. 55 (2012) 817–824.
[20] S. Isert, L. Xin, J. Xie, S.F. Son, The effect of decorated graphene addition on the burning rate of ammonium perchlorate composite propellants, Combust. Flame 183 (2017) 322–329.
[21] R. Thiruvengadathan, S.W. Chung, S. Basuray, B. Balasubramanian, C.S. Staley, K. Gangopadhyay, S. Gangopadhyay, A versatile self-assembly approach toward high performance nanoenergetic composite using functionalized graphene, Langmuir 30 (2014) 6556–6564.
[22] G.C. Egan, M.R. Zachariah, Commentary on the heat transfer mechanisms controlling propagation in nanothermites, Combust. Flame 162 (2015) 2959–2961.
[23] J. Shen, Z. Qiao, K. Zhang, J. Wang, R. Li, H. Xu, G. Yang, F. Nie, Effects of nano-Ag on the combustion process of Al-CuO metastable intermolecular composite, Appl. Therm. Eng. 62 (2014) 732–737.
[24] Y.X. Fu, Z.X. He, D.C. Mo, S.S. Lu, Thermal conductivity enhancement of epoxy adhesive using graphene sheets as additives, Int. J. Therm. Sci. 86 (2014) 276–283.
[25] K. Kakaei, One-pot electrochemical synthesis of graphene by the exfoliation of graphite powder in sodium dodecyl sulfate and its decoration with platinum nanoparticles for methanol oxidation, Carbon 51 (2013) 195–201.
[26] K.T. Sullivan, W. Chiou, R. Fiore, M.R. Zachariah, In situ microscopy of rapidly heated nano-Al and nano-Al/$WO_3$ thermites, Appl. Phys. Lett. 97 (2010) 133104.
[27] J. Wang, A. Hu, J. Persic, J.Z. Wen, Y.N. Zhou, Thermal stability and reaction properties of passivated Al/CuO nano-thermite, J. Phys. Chem. Solids 72 (2011) 620–625.
[28] T. Fujimura, S. Tanaka, In-situ high temperature x-ray diffraction study of Cu/$Al_2O_3$ interface reactions, Acta Mater. 46 (1998) 3057–3061.
[29] J.H. Shy, B.H. Tseng, Characterization of $CuAlO_2$ thin film prepared by rapid thermal annealing of an $Al_2O_3$/$Cu_2O$/sapphire structure, J. Phys. Chem. Solids 66 (2005) 2123–2126.
[30] J. Lee, S. Um, Y. Heo, J. Lee, J. Kim, Phase development and crystallization of $CuAlO_2$ thin films prepared by pulsed laser deposition, J. Eur. Ceram. Soc. 30 (2010) 509–512.
[31] K. Zhang, C. Rossi, G.A. Ardila Rodriguez, C. Tenailleau, P. Alphonse, Development of a nano-Al/CuO based energetic material on silicon substrate, Appl. Phys. Lett. 91 (2007) 113117.
[32] M. Neumann-Spallart, S.P. Pai, R. Pinto, PLD growth of $CuAlO_2$, Thin Solid Films 515 (2007) 8641–8644.
[33] A.M. Baghdasaryan, M.A. Hobosyan, H.L. Khachatryan, O.M. Niazyan, S.L. Kharatyan, L.H. Sloyan, Y.G. Grigoryan, The role of chemical activation on the combustion and phase formation laws in the Ni-Al-promoter system, Chem. Eng. J. 188 (2012) 210–215.

[34] S.M. Umbrajkar, M. Schoenitz, E.L. Dreizin, Exothermic reactions in Al-CuO nanocomposites, Thermochim. Acta 451 (2006) 34–43.
[35] K.J. Blobaum, A.J. Wagner, J.M. Plitzko, D. Van Heerden, D.H. Fairbrother, T.P. Weihs, Investigating the reaction path and growth kinetics in multilayer foils, J. Appl. Phys. 94 (2003) 2923–2929.
[36] F. Yi, J.B. DeLisio, N. Nguyen, M.R. Zachariah, D.A. LaVan, High heating rate decomposition dynamics of copper oxide by nanocalorimetry-coupled time-of-flight mass spectrometry, Chem. Phys. Lett. 689 (2017) 26–29.
[37] J.Y. Kim, J.A. Rodriguez, J.C. Hanson, A.I. Frenkel, P.L. Lee, Reduction of CuO and $Cu_2O$ with $H_2$: H embedding and kinetic effects in the formation of suboxides, J. Am. Chem. Soc. 125 (2003) 10684–10692.
[38] C.D. Wagner, W.M. Riggs, L.E. Davis, J.F. Moulder, G.E. Muilenberg, Handbook of X-Ray Photoelectron Spectroscopy, Perkin-Elmer Corporation, 1979.
[39] S. Thirumalairajan, V.R. Mastelaro, C.A. Escanhoela Jr, In-depth understanding of the relation between $CuAlO_2$ particle size and morphology for ozone gas sensor detection at a nanoscale level, ACS Appl. Mater. Interfaces 6 (2014) 21739–21749.
[40] C. Hinnen, D. Imbert, J.M. Siffre, P. Marcus, An in situ XPS study of sputter-deposited aluminium thin films on graphite, Appl. Surf. Sci. 78 (1994) 219–231.
[41] S.F. Bartolucci, J. Paras, M.A. Rafiee, J. Rafiee, S. Lee, D. Kapoor, N. Koratkar, Graphene-aluminum nanocomposites, Mater. Sci. Eng. A 528 (2011) 7933–7937.
[42] B.R. Strohmeier, D.E. Levden, R.S. Field, D.M. Hercules, Surface spectroscopic characterization of $Cu/A1_2O_3$ catalysts, J. Catal. 94 (1985) 514–530.
[43] B.K. Kwak, D.S. Park, Y.S. Yun, J. Yi, Preparation and characterization of nanocrystalline $CuAl_2O_4$ spinel catalysts by sol-gel method for the hydrogenolysis of glycerol, Catal. Commun. 24 (2012) 90–95.
[44] J. Cai, H. Gong, The influence of ratio on properties of chemical-vapor-deposition-grown p-type Cu-Al-O transparent semiconducting films, J. Appl. Phys. 98 (2005) 033707.
[45] H. Sui, L. LeSergent, J.Z. Wen, Diversity in addressing reaction mechanisms of nanothermite composites with a layer by layer structure, Adv. Eng. Mater. (2017) 1700822.
[46] F. Saceleanu, S. Atashin, J.Z. Wen, Investigation of the effects of phase transformations in micro and nano aluminum powders on kinetics of oxidation using thermogravimetric analysis, Phys. Chem. Chem. Phys. 19 (2017) 18996–19009.
[47] M. Petrantoni, C. Rossi, V. Conédéra, D. Bourrier, P. Alphonse, C. Tenailleau, Synthesis process of nanowired Al/CuO thermite, J. Phys. Chem. Solids 71 (2010) 80–83.